



## NRC Publications Archive Archives des publications du CNRC

### **Size-selected synthesis of PtRu nano-catalysts: reaction and size control mechanism**

Bock, Christina; Paquet, Chantal; Coullard, Martin; Botton, Gianluigi A.; MacDougall, Barry R.

This publication could be one of several versions: author's original, accepted manuscript or the publisher's version. / La version de cette publication peut être l'une des suivantes : la version prépublication de l'auteur, la version acceptée du manuscrit ou la version de l'éditeur.

For the publisher's version, please access the DOI link below. / Pour consulter la version de l'éditeur, utilisez le lien DOI ci-dessous.

#### **Publisher's version / Version de l'éditeur:**

<https://doi.org/10.1021/ja0495819>

*Journal of the American Chemical Society*, 126, June 25, pp. 8028-8037, 2004

#### **NRC Publications Record / Notice d'Archives des publications de CNRC:**

<https://nrc-publications.canada.ca/eng/view/object/?id=cee438e8-f8dd-42d7-88ae-6b4c5e930640>

<https://publications-cnrc.canada.ca/fra/voir/objet/?id=cee438e8-f8dd-42d7-88ae-6b4c5e930640>

Access and use of this website and the material on it are subject to the Terms and Conditions set forth at

<https://nrc-publications.canada.ca/eng/copyright>

READ THESE TERMS AND CONDITIONS CAREFULLY BEFORE USING THIS WEBSITE.

L'accès à ce site Web et l'utilisation de son contenu sont assujettis aux conditions présentées dans le site

<https://publications-cnrc.canada.ca/fra/droits>

LISEZ CES CONDITIONS ATTENTIVEMENT AVANT D'UTILISER CE SITE WEB.

#### **Questions?** Contact the NRC Publications Archive team at

PublicationsArchive-ArchivesPublications@nrc-cnrc.gc.ca. If you wish to email the authors directly, please see the first page of the publication for their contact information.

**Vous avez des questions?** Nous pouvons vous aider. Pour communiquer directement avec un auteur, consultez la première page de la revue dans laquelle son article a été publié afin de trouver ses coordonnées. Si vous n'arrivez pas à les repérer, communiquez avec nous à PublicationsArchive-ArchivesPublications@nrc-cnrc.gc.ca.



## Size-Selected Synthesis of PtRu Nano-Catalysts: Reaction and Size Control Mechanism

Christina Bock,<sup>\*,†</sup> Chantal Paquet,<sup>†</sup> Martin Couillard,<sup>‡</sup> Gianluigi A. Botton,<sup>‡</sup> and Barry R. MacDougall<sup>†</sup>

Contribution from the National Research Council of Canada, 1200 Montreal Road, Ottawa, Ontario, Canada, K1A 0R6, and Brockhouse Institute for Materials Research, McMaster University, 1280 Main Street West, Hamilton, Ontario, Canada, L8S 4L8

Received January 23, 2004; E-mail: christina.bock@nrc-cnrc.gc.ca

**Abstract:** A rapid synthesis method for the preparation of PtRu colloids and their subsequent deposition on high surface area carbons is presented. The reaction mechanism is shown to involve the oxidation of the solvent, ethylene glycol, to mainly glycolic acid or, depending on the pH, its anion, glycolate, while the Pt(+IV) and Ru(+III) precursor salts are reduced. Glycolate acts as a stabilizer for the PtRu colloids and the glycolate concentration, and hence the size of the resulting noble metal colloids is controlled via the pH of the synthesis solution. Carbon-supported PtRu catalysts of controlled size can be prepared within the range of 0.7–4 nm. Slow scan X-ray diffraction and high-resolution transmission electron microscopy show the PtRu catalysts to be crystalline. The Ru is partly dissolved in the face-centered cubic Pt lattice, but the catalysts also consist of a separate, hexagonal Ru phase. The PtRu catalysts appear to be of the same composition independent of the catalyst size in the range of 1.2–4 nm. Particular PtRu catalysts prepared in this work display enhanced activities for the CH<sub>3</sub>OH electro-oxidation reaction when compared to two commercial catalysts.

### Introduction

Pt- and PtRu-based nanoparticles are of major interest as anode catalysts for direct methanol and reformate fuel cells.<sup>1,2</sup> The latter utilizes H<sub>2</sub> as anode fuel that contains CO resulting typically from re-formation of CH<sub>3</sub>OH. Up to now, bimetallic PtRu anode catalysts have shown superior activities for these fuel cells. The oxidation of CH<sub>3</sub>OH to CO<sub>2</sub> at “low” potentials takes place via a bifunctional mechanism that involves the abstraction reaction of hydrogen through the adsorption of CH<sub>3</sub>-OH on Pt, forming a CO-type intermediate species at the catalyst surface. The complete oxidation of the adsorbed reaction intermediate to CO<sub>2</sub> is promoted by –OH-type groups that are formed via the partial oxidation of H<sub>2</sub>O on neighboring Ru sites.<sup>2</sup> A similar bifunctional mechanism applies to the H<sub>2</sub> oxidation reaction in the presence of CO. On the basis of this bifunctional mechanism, it is clear that the catalytic performance is strongly dependent on the distribution of Pt and Ru sites on the atomic level, and it is believed that alloys are most beneficial in this regard.<sup>1–5</sup> However, for the successful implementation of direct methanol fuel cells, in particular, the catalytic performance and the amount of noble metal catalysts used need to be reduced significantly. It is well known that the catalyst utilization can

be improved by supporting Pt and PtRu particles in the nanosize range on high surface area carbons.<sup>6</sup> Various methods are used for the preparation of supported catalysts, such as the impregnation of the support with the noble metal precursor salts that are subsequently reduced, typically in a hydrogen atmosphere at elevated temperatures.<sup>7</sup>

An attractive alternative route to preparing supported Pt and PtRu catalysts is the synthesis of colloidal catalyst solutions that is followed by the deposition of the nanosized catalysts on a suitable support material such as high surface area carbon blacks.<sup>8</sup> To stabilize the colloids in solution, organic stabilizers such as polyvinyl pyrrolidone that interact with the Pt and PtRu catalyst surface sites have been used.<sup>9,10</sup> Once the catalysts are deposited on the carbon black, the stabilizer molecules are preferably removed, as they otherwise hinder the access of the fuel to the catalyst sites. It has been shown that organic stabilizers can be removed by oxidative heat treatment.<sup>11</sup> However, heat treatment can alter the properties of these catalysts. In the case of PtRu alloys, it is known that heat treatments as low as 220 °C result in Pt and Ru phase

<sup>†</sup> National Research Council of Canada.

<sup>‡</sup> McMaster University.

- (1) Bockris, J. O'M.; Wroblowa, H. *J. Electroanal. Chem.* **1964**, *7*, 428–451.
- (2) Watanabe, M.; Motoo, S. *J. Electroanal. Chem.* **1975**, *60*, 267–273.
- (3) Gasteiger, H. A.; Markovic, N.; Ross, P. N.; Cairns, E. J. *J. Electrochem. Soc.* **1994**, *147*, 1795–1806.
- (4) Iwasita, T.; Hoster, H.; John-Anacker, A.; Lin, W. F.; Vielstich, W. *Langmuir* **2000**, *16*, 522–529.
- (5) Bock, C.; MacDougall, B.; LePage, Y. *J. Electrochem. Soc.*, in press.

- (6) Wilson, M. S.; Gottesfeld, S. *J. Appl. Electrochem.* **1992**, *1*, 1–7.
- (7) Richard, D.; Gallezot, P. In *Preparation of Catalysis IV*; Delmon, B., Grange, P., Jacobs, P. A., Poncelet, G., Eds.; Elsevier: Amsterdam, 1988; pp 71–81.
- (8) Schmidt, T. J.; Noeske, M.; Gasteiger, H. A.; Behm, R. J.; Britz, P.; Brijoux, W.; Boennemann, H. *Langmuir* **1997**, *13*, 2591–2595.
- (9) Dalmia, A.; Lineken, C. L.; Savinell, R. F. *Colloid Interface Sci.* **1998**, *205*, 535–537.
- (10) Bonet, F.; Delmas, V.; Grugeon, S.; Urbina, R. H.; Silvert, P. Y.; Tekaiia-Elhissien, K. *Nanostruct. Mater.* **1999**, *11*, 1277–1284.
- (11) Dubeau, L.; Coutanceau, C.; Garnier, E.; Leger, J. M.; Lamy, C. *J. Appl. Electrochem.* **2003**, *33*, 419–429.

separation.<sup>5</sup> This in turn alters the surface concentration and distribution of Pt and Ru, typically resulting in lower catalyst activities.

In this work, a simple chemical reduction route is discussed that results in the formation of PtRu nanoparticles that can be supported on substrates such as high surface area carbons. The synthesis method can be used to prepare PtRu catalysts selectively in the nanoscale particle size range of less than 4 nm without changing the composition of the PtRu catalysts. The mechanism of the PtRu colloid formation reaction is discussed, and PtRu nano-catalysts deposited on high surface area carbons are characterized using X-ray diffraction, X-ray photon spectroscopy, and transmission electron microscopy (TEM). The activities of carbon-supported PtRu particles for the electrochemical CH<sub>3</sub>OH oxidation reaction are also discussed and compared to those of commercial PtRu catalysts.

## Experimental Section

**Preparation of Carbon-Supported PtRu Catalysts.** The synthesis of the bimetallic PtRu colloids was carried out in ethylene glycol (Anachemia) solutions containing different concentrations of sodium hydroxide (EM Science). First, 0.2326 g of PtCl<sub>4</sub> (Alfa Aesar, 99.9% metals basis) and 0.1383 g of RuCl<sub>3</sub> (Alfa Aesar, 99.9% metals basis) were dissolved in 50 mL of ethylene glycol containing between 0.2 and 0.04 M NaOH. The solutions were stirred for 30 min in air at room temperature, subsequently heated under reflux to 160 °C for 3 h, and then cooled in air. Temperatures of 160 °C were achieved within less than 20 min. Dark brown solutions containing the PtRu colloids were formed in this manner and are referred to as colloidal solutions in this work. Appropriate aliquots of the colloidal solutions were mixed with carbon blacks in a large and open beaker for up to 24 h, resulting in the deposition of the PtRu colloids on the carbon substrates, Vulcan XC-72R (Cabot). The carbon-supported PtRu catalysts were then filtered and extensively washed with water. Initial, that is, undiluted, filtrate solutions were analyzed for organic acids using high performance liquid chromatography (HPLC). The carbon-supported PtRu catalysts were generally dried at 160 °C in air for 1 h. A mortar was used to homogeneously ground the carbon-supported catalyst powders. The supported catalysts were stored in air at room temperature and were found to have a shelf life of at least 1 year. Prior to the synthesis of the colloidal solutions, the PtCl<sub>4</sub> and RuCl<sub>3</sub> were dried in an air oven at 135 °C. The ethylene glycol was dried using molecular sieves type 3a (BDH), while the carbon black powder was used as received.

**Instrumentations/Techniques.** XPS spectra were obtained using a PHI 5500 spectrometer equipped with a monochromatized Al K $\alpha$  source. The data were collected using an aperture of 4, a 70° takeoff angle, and a pass energy of 23.50 eV. The position of the C 1s peak, that is, 284.6 eV, was used to correct the binding energies for all catalysts for possible charging effects. The catalyst powders were attached to conductive carbon tape for the XPS analyzes. For each catalyst, a survey spectrum was collected before high-resolution spectra were recorded. Deconvolutions of the XPS spectra were performed using a Grams\_32 Spectral Note base software program. A Philips CM 20 TEM was employed to measure the size of the PtRu catalysts. A JEOL 2010F operated at 200 keV and equipped with an energy-dispersive X-ray spectrometer (EDS) and a Gatan annular dark-field (ADF) detector was also employed. For the TEM analyses, the carbon-supported catalyst powders were ultrasonically suspended in ethanol, and a drop of the catalyst powder suspension was applied to a holey amorphous carbon film on a 300 mesh Cu grid (Marivac, Limited). A Scintag XDS2000 system was employed using a Cu K $\alpha$  source to obtain XRD spectra of the carbon-supported catalysts. The angle extended from 20° to 80° and varied using a step size of 0.06°, accumulating data for 60 s per step. Silicon powder (typically 1–20  $\mu$ m, 99.9985%

purity, Alfa Aesar) that was homogeneously grounded with the carbon-supported catalysts was used as an internal standard. XRD spectra of the Si-free and Si-containing samples were obtained for all catalysts. The software program Topas 2 (DIFFRAC<sup>PLUS</sup> Topas, Bruker axs, Inc.) was employed to extract lattice parameter constants from the experimental XRD spectra. The entire XRD spectra were employed to analyze the data. The XRD, XPS, and TEM characterizations were carried out on the unused, that is, as-prepared, catalyst powders. All electrochemical experiments were carried out using a Solartron SI 1287 electrochemical interface (Solartron Group, Ltd.) driven by the Corrware software program (Scribner, Assoc.). Undiluted filtrates of the colloidal synthesis solutions were analyzed for carboxylic acids using a HP series 1100 HPLC. An ion-interaction column (Mandel), thermostated at 46 °C, was used. The UV detector was set at 195 nm. 0.01 M H<sub>2</sub>SO<sub>4</sub> was used as the mobile phase at a flow rate of 0.3 mL min<sup>-1</sup>. A Fisher Accumet pH meter, model 805 MP, and a combined glass pH electrode (Corning) were used for pH measurements. A digital Mirak hotplate was used for the synthesis of the colloids that allowed controlled stirring and heating conditions.

**Electrochemical Measurements.** Three-compartment cells, in which the reference electrode was separated from the working and counter electrode compartment by a Luggin capillary, were employed for the electrochemical studies. The cells were equipped with a water jacket and condensers for the electrochemical oxidation studies that were carried out at 60 °C. A large surface area Pt gauze served as counter electrode, and a saturated calomel electrode (SCE) was used as the reference electrode. All potentials in this study are reported with respect to the SCE. The catalyst powders were formed into electrodes by sonicating 13 mg of the carbon-supported catalyst powders in 1 mL of H<sub>2</sub>O and 300  $\mu$ L of Nafion solution (5 wt %, Aldrich) for 15 min, forming a catalyst ink. Subsequently, 10  $\mu$ L of catalyst ink was applied to form a thin layer of ca. 0.5 cm<sup>2</sup> geometrical area on a gold foil (0.5  $\times$  2  $\times$  0.1 cm<sup>3</sup>, Goodfellow, 99.95% metal basis). The catalyst layer was then dried at 80 °C in an air oven for 30 min. Electrical contact was made by firmly attaching an Au wire via a small hole to the Au foil. Commercially available carbon-supported PtRu catalysts were also tested for their CH<sub>3</sub>OH electro-oxidation activity. 20 wt % Pt and 10 wt % Ru catalysts supported on carbon black (Vulcan XC72-R) were obtained from Alfa Aesar and E-Tek, Inc.

**Solutions and Chemicals.** All chemicals used in this work were A.C.S. grade, and high resistivity 18 M $\Omega$  H<sub>2</sub>O was used. Methanol oxidation studies were carried out in deoxygenated 0.5 M H<sub>2</sub>SO<sub>4</sub> + 0.5 M CH<sub>3</sub>OH solutions.

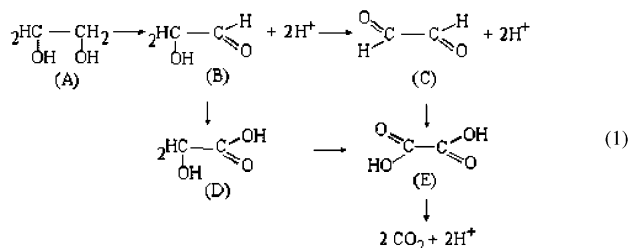
## Results and Discussion

**Synthesis of Bimetallic PtRu Colloids in Ethylene Glycol Solutions.** The synthesis of monometallic noble metal colloids in ethylene glycol solution has been suggested in previous work.<sup>9,10</sup> Various monometallic noble metal colloids were synthesized in ethylene glycol using organic stabilizers such as poly(*N*-sulfonatopropyl *p*-benzamide)<sup>9</sup> and polyvinyl pyrrolidone (PVP).<sup>10</sup> The synthesis of monometallic colloids in ethylene glycol solution of alkaline pH (>12) without the addition of a stabilizer molecule has also been discussed.<sup>12</sup> It was proposed that the noble metal precursor salts such as H<sub>2</sub>PtCl<sub>6</sub> are reduced by nitrogen passed through the ethylene glycol solution and that stabilizer-free, that is, “unprotected”, colloids were prepared. The colloids were suggested to be solely stabilized by the “dielectric” properties of the ethylene glycol solvent. In the following sections, the size-selected synthesis of bimetallic PtRu colloids in ethylene glycol solutions is discussed. The reaction mechanism and the stabilization of the colloidal particles are

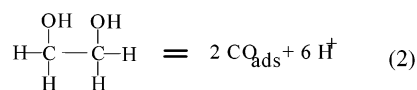
(12) Wang, Y.; Ren, J.; Deng, K.; Gui, L.; Tang, Y. *Chem. Mater.* **2000**, *12*, 1622–1627.

investigated in detail. It should be noted that ethylene glycol is an alcohol and is readily oxidized. Therefore, ethylene glycol is more likely to act as a reducing agent for the Pt and Ru precursor salts rather than nitrogen that is generally utilized to remove oxygen from solutions. Furthermore, oxidation products resulting from the ethylene glycol oxidation reaction could interact with the noble metal colloids and hence act as their stabilizers.

**Reaction Mechanism: Reduction of the Precursor Salts Accompanied by the Oxidation of Ethylene Glycol.** Ethylene glycol is an alcohol and a very weak acid ( $pK_a \approx 15^{13}$ ) that can be oxidized to aldehydes, carboxylic acids, and  $CO_2$ , as shown in the following reaction scheme:



For this reaction pathway to take place, the  $-OH$  groups of ethylene glycol (A) interact with Pt- and Ru-ion sites, resulting in the oxidation of the alcohol groups to aldehydes (B and C). These aldehydes are not very stable and are easily oxidized to glycolic (D) and oxalic acid (E), respectively. The two carboxylic acids may be further oxidized to  $CO_2$  or carbonate in alkaline media. The electrons donated from these oxidation reactions result in the reduction of the Pt and Ru metal ions. It is also well known that platinum is an excellent catalyst to abstract hydrogen from carbon atoms.<sup>14</sup> Therefore, the oxidation of ethylene glycol could take place via an alternative or parallel reaction pathway that involves the hydrogen abstraction from the carbon atoms of ethylene glycol by platinum, as shown in eq 2:



This reaction pathway results in the adsorption of CO ( $CO_{\text{ads}}$ ) on platinum that may be further oxidized to  $CO_2$ . In parallel work, we prepared Pt colloids via this ethylene glycol synthesis route and deposited the colloids on Au and Teflon substrates.<sup>15</sup> Infrared studies confirmed the presence of linearly adsorbed CO as well as carboxylic acids on the electrode surface, thus suggesting that ethylene glycol oxidation takes place via both pathways, eqs 1 and 2. The infrared data also support the view that oxidation products containing carboxyl groups act as stabilizers for these colloids. Furthermore, it was shown that these organics,  $CO_{\text{ads}}$ , and carboxyl groups can be removed either by electrochemical oxidation or by oxidative heat treatment at “low” temperatures ( $<160$  °C), thus freeing up catalyst surface sites without changing the properties of the PtRu catalysts.<sup>5,15</sup> To establish the reaction mechanism and analyze the dominating reaction pathway, HPLC analysis of the synthesis

solutions was carried out after the PtRu colloids were adsorbed on carbon, that is, in the final synthesis solution, as described in the Experimental Section. Both oxalic and glycolic acids were detected in the chromatograms with retention times of 4.2 and 7.2 min, respectively. The presence of these two species in the final synthesis solution confirms that ethylene glycol is at least partly oxidized according to the reaction scheme shown in eq 1. The oxalic and glycolic acid concentrations in the final synthesis solution were determined as  $6 \times 10^{-5}$  and  $1.5 \times 10^{-2}$  M, respectively, independent of the NaOH concentration. The quantitative analysis indicates that glycolic acid is the dominating product of the ethylene glycol oxidation reaction. The oxidation of one ethylene glycol molecule to one oxalic and one glycolic acid molecule yields 8 and 4 electrons, respectively. This suggests that “electron concentrations” of at least  $5 \times 10^{-4}$  and  $6 \times 10^{-2}$  M, respectively, are generated by the oxidation of ethylene glycol to these two acids. The reduction reactions of the  $1.4 \times 10^{-2}$  M  $Ru^{3+}$  and  $1.4 \times 10^{-2}$  M  $Pt^{4+}$ , if reduced to metals, require electron concentrations of  $4.2 \times 10^{-2}$  and  $5.6 \times 10^{-2}$  M, respectively. Therefore, the complete reduction of the two noble metal precursor salts to metals requires a total electron concentration of  $9.8 \times 10^{-2}$  M, of which at least  $6 \times 10^{-2}$  M, that is, more than 60%, are produced by the oxidation of ethylene glycol to glycolic acid. This suggests that the majority of the electrons needed for the noble metal salt reduction are provided by the oxidation of ethylene glycol to glycolic acid.

**Adjustment of the PtRu Particle Size.** The glycolic acid concentration of  $1.5 \times 10^{-2}$  M found in the final synthesis solution is comparable to the precursor salt concentration, and hence this molecule could be the stabilizer of the PtRu colloids, as discussed in this section. The dissociation constant of glycolic acid is  $1.48 \times 10^{-4}$  mol  $L^{-1}$  at 25 °C;<sup>13</sup> that is, glycolic acid is present in its deprotonated form as the glycolate anion,  $A^-$ , in alkaline solutions and in its protonated form, HA, in acidic solutions. Glycolate is believed to act as a good stabilizer for the colloids, possibly forming chelate-type complexes via its carboxyl groups. Such interactions between the PtRu catalysts and the neutral, acidic form, that is, glycolic acid, are smaller, and glycolic acid is believed to be a poor stabilizer. Therefore, the pH of the synthesis solution is expected to greatly influence the stability and size of the resulting colloids, in the range where the glycolate concentration changes. The theoretical concentrations of the HA and  $A^-$  species as a function of pH are shown in Figure 1. An initial glycolic acid concentration of  $1.5 \times 10^{-2}$  M and the dissociation constant of  $1.48 \times 10^{-4}$  mol  $L^{-1}$  were used for the calculation. Changes in the glycolate and glycolic acid concentrations are seen to take place within the pH range between 6 and 2. At pH values higher than 6, a constant glycolate concentration is reached, while below pH 2, glycolate is essentially nonexistent. On the basis of these data, and assuming that glycolate acts as stabilizers, the PtRu catalyst size is expected to be the smallest and essentially independent of the solution pH when larger than 6. The catalyst size is further expected to continuously increase with decreasing pH in the pH range from 6 to 2, and again to be essentially independent of the solution pH, with, however, larger particle sizes at pH values less than 2.

This proposed pH influence on the resulting PtRu catalyst size was tested by adjusting the pH of the synthesis solution

(13) *CRC Handbook of Chemistry and Physics*, 71st ed.; Lide, D. R., Ed.; CRC Press: Boston, 1990.

(14) Bagotsky, V. S.; Vassiliev, Y. B. *Electrochim. Acta* **1967**, *12*, 1323–1343.

(15) Bock, C.; Krasinski, A.; MacDougall, B., in preparation.



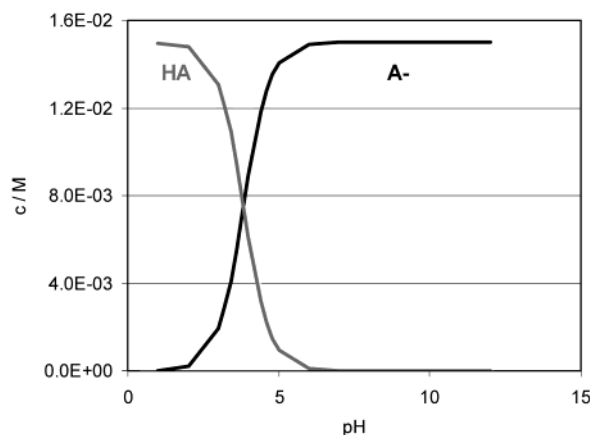


**Figure 1.** Dependence of glycolic acid (HA; gray line) and glycolate ( $A^-$ , black line) concentration on the pH for a total HA +  $A^-$  concentration of  $1.5 \times 10^{-2}$  M. The acid dissociation constant ( $K_D$ ) value of  $1.48 \times 10^{-4}$  mol  $L^{-1}$ <sup>13</sup> was used for the calculation.

**Table 1.** Influence of the NaOH Concentration on the Resulting PtRu Particle Size<sup>a</sup>

$C_{NaOH}/mol\ L^{-1}$	initial pH <sup>b</sup>	final pH <sup>c</sup>	PtRu particle size <sup>a</sup> /nm
0.1	~11.1	~6	$0.7 \pm 0.5$
0.085	~10.5	5.5	$1.2 \pm 0.5$
0.075	~10	5	$1.5 \pm 0.8$
0.071	~9.5	4.5	$2 \pm 0.8$
0.069	~7.8	4	$2.2 \pm 0.8$
0.068	~7.5	3.5	$3 \pm 1.5$
0.063	~7.2	3.3	$4 \pm 1.5$

<sup>a</sup> PtRu particle sizes were estimated from TEM images obtained for carbon-supported catalysts. <sup>b</sup> pH of the not yet heated synthesis solutions measured 30 min after dissolving the noble metal precursor salts in the ethylene glycol + NaOH solutions. <sup>c</sup> pH of the synthesis solutions that were heated at 160 °C for 3 h. The solutions were cooled to room temperature prior to the pH measurements.

using different NaOH concentrations, as listed in Table 1. The pH of the freshly prepared, that is, not yet heated, solutions was found to decrease rapidly and reach a steady-state value within ca. 30 min. The steady-state values of a particular solution containing the noble metal salts were always lower than those measured for ethylene glycol solutions of corresponding NaOH concentration, that is, in the absence of the noble metal salts, indicating the influence of these two salts that are present in high concentrations on the solution pH. Using this NaOH concentration range, the pH of the unheated synthesis solution was varied between ca. 11 and 7. In all cases, the initial pH value dropped by 4–5 orders of magnitude as a result of the reduction of the noble metal salts at higher temperatures. The drop in solution pH is consistent with the reaction schemes shown in eqs 1 and 2.

The resulting particle size and particle size distributions obtained from TEM images for the PtRu colloids synthesized using the different NaOH concentrations are shown in Table 1 and Figure 2. All TEM images were obtained for carbon-supported PtRu catalysts. The data suggest that the size of the PtRu catalysts can be controlled by varying the NaOH concentrations between ca. 0.1 and 0.06 M. It is seen that the catalyst sizes change within the (final) solution pH range between 6 and 3. This is the same pH range where the glycolate concentration changes, consistent with the view that glycolate acts as a stabilizer for the PtRu colloids. The size of the PtRu catalysts prepared using solutions of higher pH values, that is, a final solution pH more positive than 6, was found to be

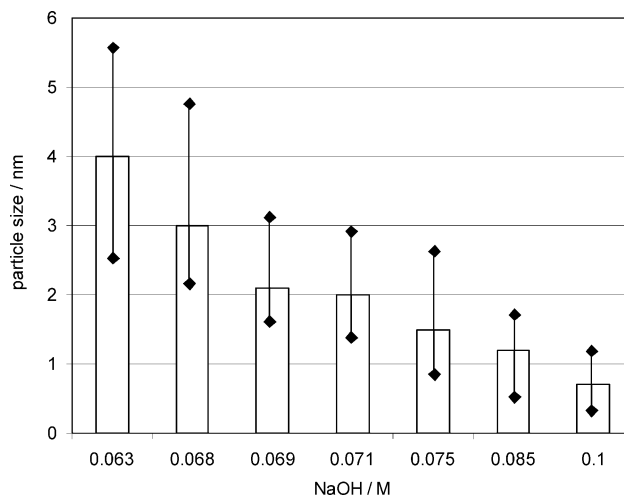


**Figure 2.** Average particle size dependence on the NaOH concentration in the ethylene glycol synthesis solution for initial  $1.4 \times 10^{-2}$  M  $PtCl_4$  +  $1.4 \times 10^{-2}$  M  $RuCl_3$  solutions. The particle size distributions characteristic for the particles synthesized using a particular NaOH concentration are indicated by the vertical lines and diamonds. The particle sizes were extracted from TEM images obtained for PtRu catalysts supported on Vulcan XC-72R.

essentially independent of the solution pH, while the use of lower NaOH concentrations, which resulted in final solution pH values of less than 3, resulted in significantly larger PtRu particles that were in fact solid powders rather than colloidal solutions. These results are also consistent with the view that glycolate acts as a stabilizer for the PtRu colloids. Furthermore, the results show that the synthesis solution pH is a key factor that influences the catalyst particle size. The possibility of the reaction of the carboxylic acids and the ethylene glycol to form an ester has not been investigated. The quantity of esters formed would be smaller than the estimated amount of glycolic acid. An ester could potentially act as a stabilizer for the PtRu particles. However, the control of its ability to stabilize the particles and hence control the particle size would not be pH dependent (unlike the situation with glycolic acid).

Acidifying “prepared” colloidal solutions to pH values of less than 2, by adding small amounts of concentrated  $H_2SO_4$ , had no effect on the properties of the PtRu catalysts deposited on carbon black from these solutions. This indicates that once the colloids have been synthesized, they are no longer influenced by changes in solution pH. The important factor is the solution pH during the “synthesis” (i.e., preparation) process. It is important to note that the particle size/pH correlation reported here is characteristic of the conditions used in this work. The use of different noble metal concentrations influences the solution pH and hence is expected to yield PtRu catalysts of different particle sizes; thus, the NaOH concentration will need to be adjusted accordingly. Furthermore, the possibility of particle size control due to electrostatic effects introduced by the different amounts of NaOH added can be ruled out. This has been confirmed in separate PtRu catalyst synthesis experiments, where  $H_2PtCl_6$  instead of  $PtCl_4$  was used. This use of the platonic acid instead of  $PtCl_4$  lowers the pH and increases the ionic strength of the synthesis solution. The resulting PtRu particle sizes were found to be conclusively larger than those for PtRu particles synthesized in a correspondingly more alkaline solution made using  $PtCl_4$  under otherwise the same conditions. This confirms that the pH and not the ionic strength of the

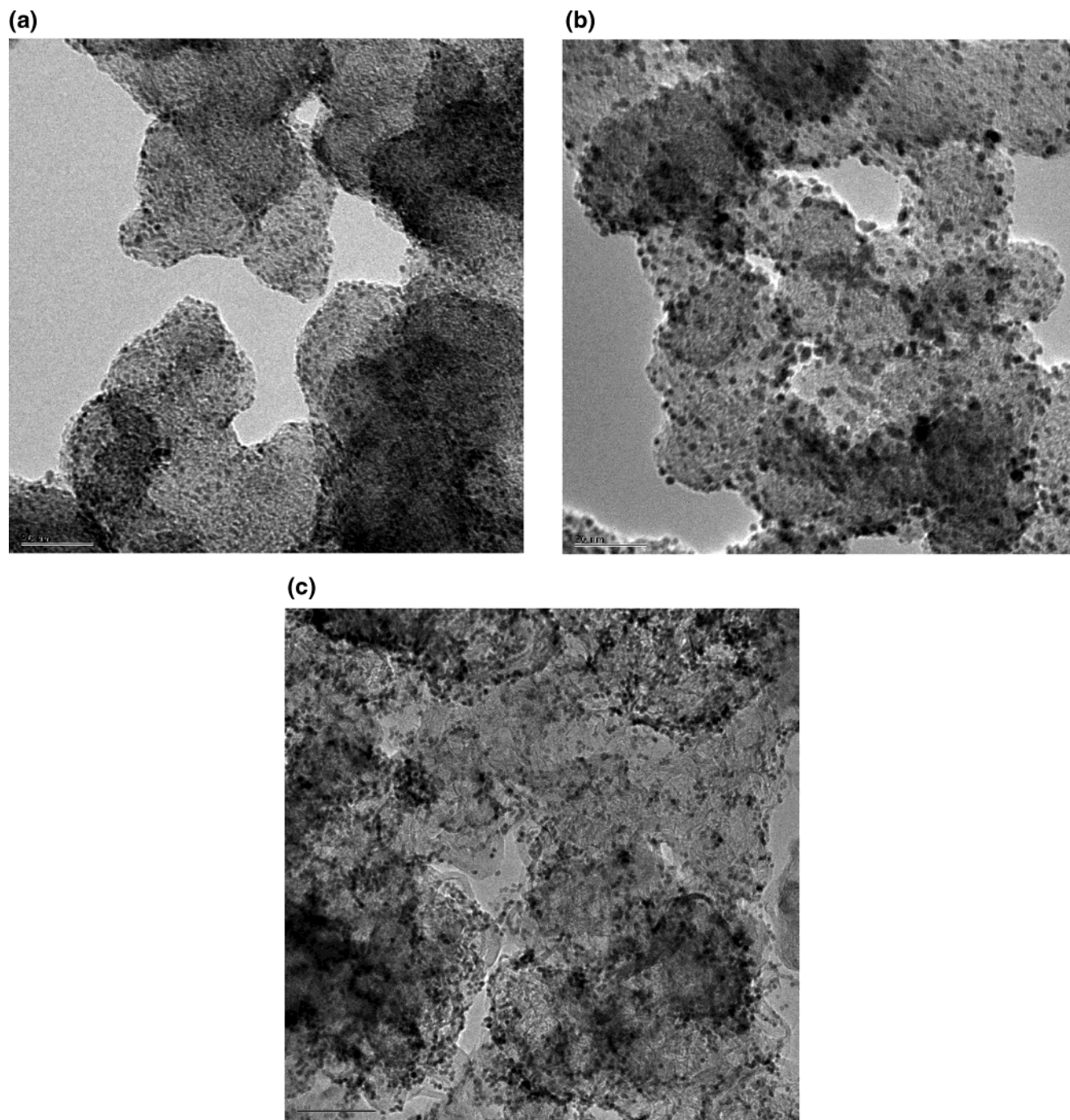


**Figure 3.** TEM images of 6 wt % Pt and 3 wt % Ru catalysts deposited on Vulcan XC-72R. The PtRu catalysts were synthesized in ethylene glycol solutions using initial  $1.4 \times 10^{-2}$  M  $\text{PtCl}_4 + 1.4 \times 10^{-2}$  M  $\text{RuCl}_3$  and the following NaOH concentrations: 0.1 M (a), 0.075 M (b), and 0.068 M (c). The bars in (a) and (b) indicate a 20 nm scale, and the bar in (c) indicates a 50 nm scale; that is, the following magnifications were used to obtain the TEM images: 1075 kx (a and b) and 470 kx (c).

synthesis solution is the controlling factor for the particle size. Figure 3a–c shows examples of TEM images obtained for PtRu particles supported on carbon black. The PtRu particles were synthesized using the following NaOH concentrations: (a) 0.1, (b) 0.075, and (c) 0.068 M. The corresponding histograms are shown in Figure 4a–c. It is seen that the NaOH concentration clearly influences the PtRu particle size, indicating that the NaOH concentration can be used to prepare PtRu nanoparticles of selected size. The size can be controlled in the range of 0.7–4 nm. It should, however, be noted that the particle size distribution is broader for the larger PtRu particles that are synthesized

using lower NaOH concentrations, as indicated in the vertical size range bars shown in Figure 2.

Changes in the synthesis solution pH during the reduction of the noble metal salts give an indication of the completion of the reaction. For the heating conditions used in this work, the synthesis solution pH was observed to drop rapidly upon heating and to reach a steady state after ca. 5 min. Within this time period, the synthesis solution temperature approached 130 °C. The fact that a steady-state pH was reached within 5 min suggests that the reduction reaction is complete within this very short time period. It is obvious that changes in the synthesis

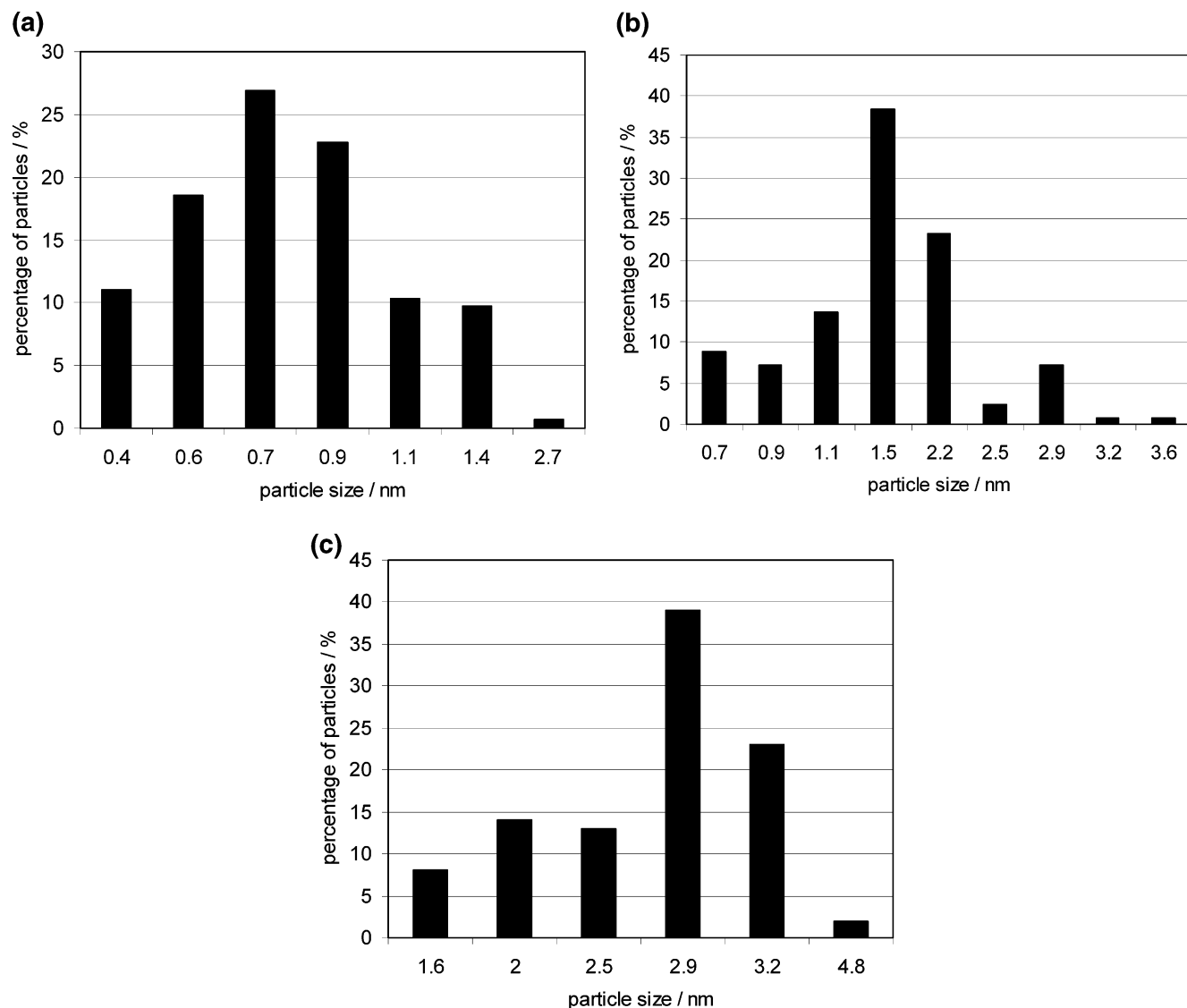


**Figure 4.** Histograms to TEM images shown in Figure 3a–c.

solution temperature and/or rate of heating will affect the reaction rate as well as the characteristics of the resulting particles such as their size. The examination of the exact influence of the temperature and heating rate on the resulting particle characteristics was not within the scope of this work and is not further discussed here. Furthermore, for all Pt–Ru particles synthesized in this work, the Pt:Ru ratio was found to be the same. The Pt:Ru ratio of the final catalysts was also the same as the Pt:Ru ratio of the precursor salts, that is, 50:50 atom %, as confirmed by EDX measurements.

**Characterization of the Carbon-Supported PtRu Catalysts: (a) XRD Characterization.** Figure 5 shows slow scan XRD spectra obtained for a range of carbon-supported PtRu catalysts of different sizes. Figure 5a shows the XRD spectra for the larger PtRu catalysts ( $>1.2$  nm), while Figure 5b shows the same for smaller ( $<1$  nm) PtRu catalysts. In the XRD spectra of the larger PtRu particles, the diffraction peaks of the face-centered cubic (fcc) Pt lattice, particularly the highest intensity Pt(111) plane, are clearly recognizable in all spectra. Due to the small particle size of these catalysts, the diffraction peaks are very broad. In fact, the peaks broaden as the particle size decreases as predicted by Scherrer's equation.<sup>16</sup> Particle size

values extracted from XRD are not listed here, as accurate particle sizes measurements from XRD data are questionable and, in fact, proper particle size measurements require TEM analysis, as carried out in this work. Overall, the XRD spectra of the larger sized catalysts (Figure 5a) are seen to be identical with the exception of the Pt diffraction peak widths. Diffraction peaks for Ru for the larger ( $>1.2$  nm) catalysts were not observed in the raw XRD data that were collected with and without the Si standard. The “absence” of diffraction peaks typical for Ru can be due to a number of reasons such as Ru not being dissolved in the Pt lattice, that is, forming a PtRu alloy, and/or the Ru being present in the amorphous form, as further discussed below. The position of the Pt(111) peak for the larger ( $>1.2$  nm) sized catalysts is shifted to higher  $2\theta$  positions than that for pure Pt that has a maxima at  $39.7645^\circ$ .<sup>17</sup> This indicates that Ru is at least partially dissolved in the Pt fcc lattice. Lattice parameter values for the Pt fcc phase ( $a_{\text{Pt}}$ ) were obtained by fitting the entire XRD spectra using the Topas

(16) Cullity, B. D. *Elements of X-ray Diffraction*; Addison-Wesley Publishing Co., Inc.: Reading, MA, 1956; p 150.

(17) *X-ray Diffraction Database*; Diffraction Management System for Windows NT; Scintag, Inc.: Cupertino, CA, 1997.



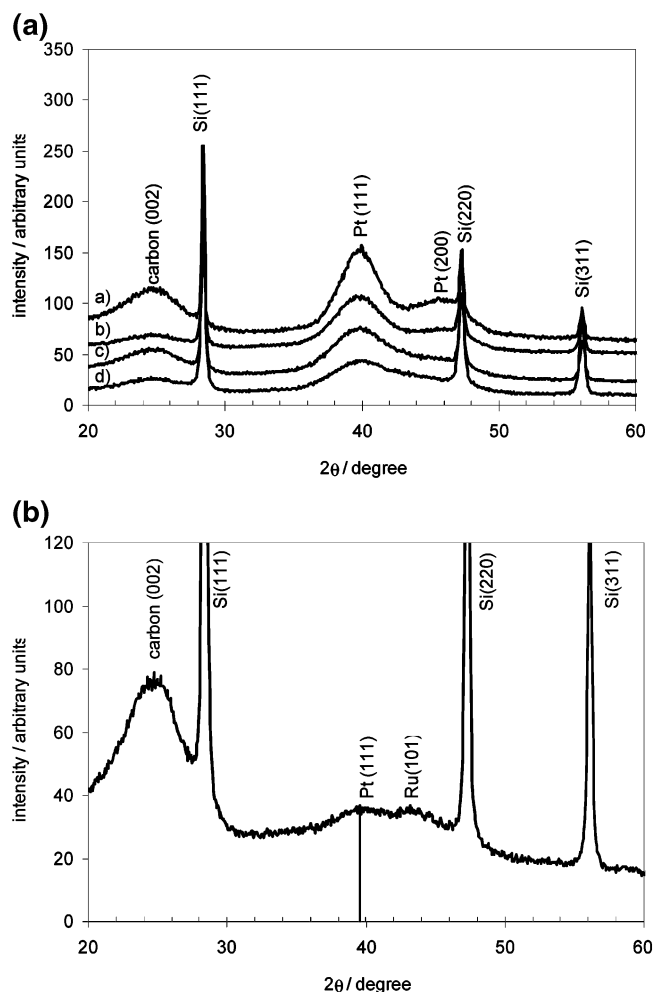


**Figure 5.** Slow scan XRD spectra for carbon-supported PtRu catalysts. Si powder was added to the catalysts as internal standard. Part a shows the XRD spectra for the larger than 1.2 nm particles, as follows: (a) 4, (b) 3.2, (c) 2.2, and (d) 1.5 nm average particle size, while part b shows an example of an XRD spectrum for smaller carbon-supported PtRu particles of 0.7 nm average size. The spectra were collected between  $2\theta$ 's of  $20^\circ$  and  $70^\circ$ , using an acquisition time of 60 s and a step size of  $0.06^\circ$ .

2 computer program. For these PtRu particles, an  $a_{\text{Pt}}$  lattice parameter value of  $0.3906 \pm 0.001$  nm was estimated. This lattice parameter value could indicate that a PtRu alloy phase of Pt:Ru atom % ratio of 85:15 ( $\pm 8\%$ ) is formed. It should be noted that this value is estimated using a Vegard's law relationship established for unsupported, that is, bulk, PtRu alloys.<sup>5</sup> Possible influences of the support on the lattice structure of these nanosized Pt-based catalysts are not accounted for in this relationship. However, such influences are expected to be small for the systems studied here, as the majority of the particles are of sizes for which more atoms are in the bulk than on the surface. Furthermore, XRD data for PtRu catalysts of 1.2 nm, size deposited on different substrates such as Si and  $\text{WO}_x$  powders, yielded the same  $a_{\text{Pt}}$  value as estimated for the carbon black substrates. This supports the use of Vegard's law relationship established for bulk alloys to estimate the lattice parameter values for the supported catalysts discussed here. The  $a_{\text{Pt}}$  value estimated from the raw XRD data was found to be independent of the particle size for the larger ( $>1.2$  nm) particles, although it should be noted that the error in the estimated lattice value increases to  $\pm 8\%$  as the particle size decreases. It is important to note that best fits of the experimental

XRD spectra were only obtained considering a Pt fcc as well as a hexagonal Ru phase. The need for a Ru phase to fit the data indicates that the Ru is indeed not entirely dissolved in the Pt fcc lattice, consistent with the less than 50 (i.e., the suggested 15) atom % Ru dissolved in the Pt fcc lattice. In all cases, the extracted lattice parameters for the hexagonal Ru phase were  $a = 0.27$  nm and  $c = 0.43$  nm, respectively; while the error of these values was high, that is,  $\pm 0.01$  nm, the values are close to those reported in the literature for bulk Ru metals.<sup>17</sup>

The diffraction peaks of the smaller PtRu particles (Figure 5b) are very broad and of low intensity, as is expected for these very small particles. However, diffraction peaks are recognizable at  $2\theta$  values of ca.  $39.8^\circ$  and  $44^\circ$ , suggesting the presence of Pt(111) as well as Ru(101) planes, respectively. The presence of the Ru(101) plane indicates that the Ru is not, at least entirely, dissolved in the Pt fcc lattice. It is unclear whether a partial PtRu alloy formation takes place for these very small catalyst particles. The  $2\theta$  position of the Pt(111) diffraction peak appears to be shifted to lower values typical for a Pt-only phase of  $39.7645^\circ$ . However, exact values cannot be obtained from these spectra due to the broad nature of the diffraction peaks of these very small catalyst particles.

**(b) XPS Characterization.** Figure 6a and b shows the XPS spectra for the Pt 4f and Ru 3p, respectively, core level regions for PtRu colloids of 2 nm size (synthesized using a 0.071 M NaOH solution). The colloids were deposited on Vulcan XC-72R, resulting in loadings of 18 wt % of Pt and 9 wt % of Ru per carbon. The less intense Ru 3p region was analyzed instead of the main Ru 5d spectra, as the latter overlays with the carbon 1s region. The results obtained by deconvoluting the XPS spectra are summarized in Table 2. The Pt core level region was deconvoluted, as described by Bancroft et al.,<sup>18</sup> while other literature sources<sup>19,20</sup> were used for the Ru 3p region. The mean free path values for Pt and Ru are in the range of 1.5 nm, and hence the XPS data for the small particles analyzed here are believed to yield data for the entire particle and not only for the surface species. It is noteworthy that the survey XPS spectra did not show the presence of  $\text{Cl}^-$ , as no peak at 198 eV typical for the highest intensity Cl 3p core level was observed.<sup>20</sup> The XPS data suggest that 38% of the Pt is present as Pt metal and 35% is present as two valent Pt-oxide, PtO, which can be reduced electrochemically. A fraction, 27%, of the Pt is also present in a higher oxidation state, likely as platinum-dioxide, PtO<sub>2</sub>. The deconvolution of the Ru 3p core level region was more difficult, due to its low intensity and hence increased contribution of noise. However, a large fraction, ca. 70%, of the Ru is suggested to be present as Ru metal, and a smaller fraction, ca. 30%, is present in a higher oxidation state, likely RuO<sub>2</sub>. It is not known whether the "partial" oxidation of both Pt and Ru takes place after the synthesis of the catalysts as colloids, for example, when the carbon-supported PtRu colloids are dried in and exposed to air and/or if the reduction reaction of the noble metal precursor salts is incomplete. The amount of RuO<sub>2</sub> is seen to be very small, possibly explaining its absence in XRD spectra as well as the possibility that the RuO<sub>2</sub> may be amorphous.

(18) Bancroft, G. M.; Adams, I.; Coatsworth, L. L.; Bennowitz, C. D.; Brown, J. D.; Westwood, W. D. *Anal. Chem.* **1975**, *47*, 586–588.

(19) Biloen, P.; Pott, G. T. *J. Catal.* **1973**, *30*, 169–178.

(20) Wagner, C. D. *Handbook of X-ray Photoelectron Spectroscopy*; Perkin-Elmer Corp., Physical Electronics Division: Eden Prairie, MN, 1979.



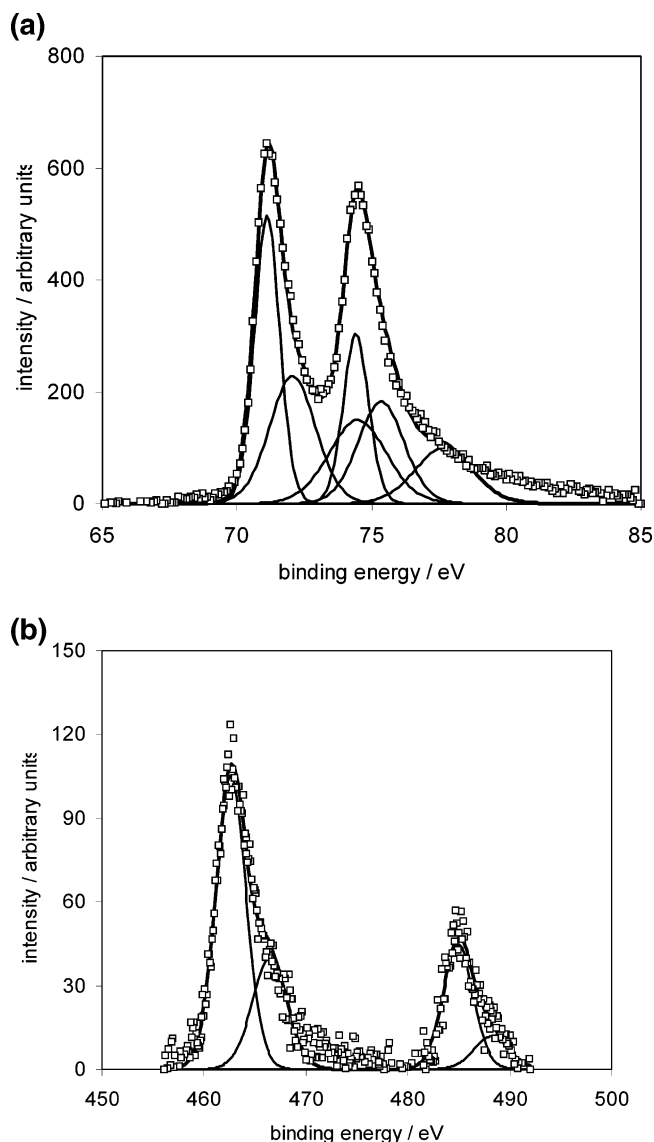


**Figure 6.** XPS core level spectra for the Pt 4f (a) and Ru 3p (b) regions of a PtRu catalyst of 2 nm average particle size supported on Vulcan XC-72R. The thick line shows the raw XPS, while the thin lines show the peaks obtained by deconvoluting the raw XPS data and the squares show the sum of the deconvoluted spectra.

**Table 2.** Binding Energies of Pt and Ru Species Obtained from Curve-Fitted XPS Spectra for Carbon-Supported PtRu<sup>a</sup> Catalysts

species	orbital/spin	binding energy/eV	peak half width/eV	assignment	relative concentrations/% <sup>b</sup>
Pt	4f <sub>7/2</sub>	71.1	1.1	Pt metal	24
	4f <sub>5/2</sub>	74.4	1.1	Pt metal	14
	4f <sub>7/2</sub>	72.1	2	PtO	20
	4f <sub>5/2</sub>	75.4	2	PtO	15
	4f <sub>7/2</sub>	74.5	2.5	PtO <sub>2</sub>	16
	4f <sub>5/2</sub>	77.7	2.5	PtO <sub>2</sub>	11
Ru	3p <sub>1/2</sub>	462.4	3.3	Ru metal	47
	3p <sub>3/2</sub>	484.8	3.3	Ru metal	24
	3p <sub>1/2</sub>	466.1	4	RuO <sub>2</sub>	23
	3p <sub>3/2</sub>	488.6	4	RuO <sub>2</sub>	6

<sup>a</sup> PtRu catalyst (2 nm average particle size) deposited on Vulcan XC-72R. 20 wt % Pt and 10 wt % Ru per carbon. <sup>b</sup> Relative concentrations are equal to the corresponding, deconvoluted peak areas divided by the total XPS signal area extracted from the experimental XPS core level regions of either Pt 4f or Ru 3p.

(c) **Scanning TEM Images and EDS Analyses.** Figure 7a shows an annular dark field (ADF) image taken in the scanning

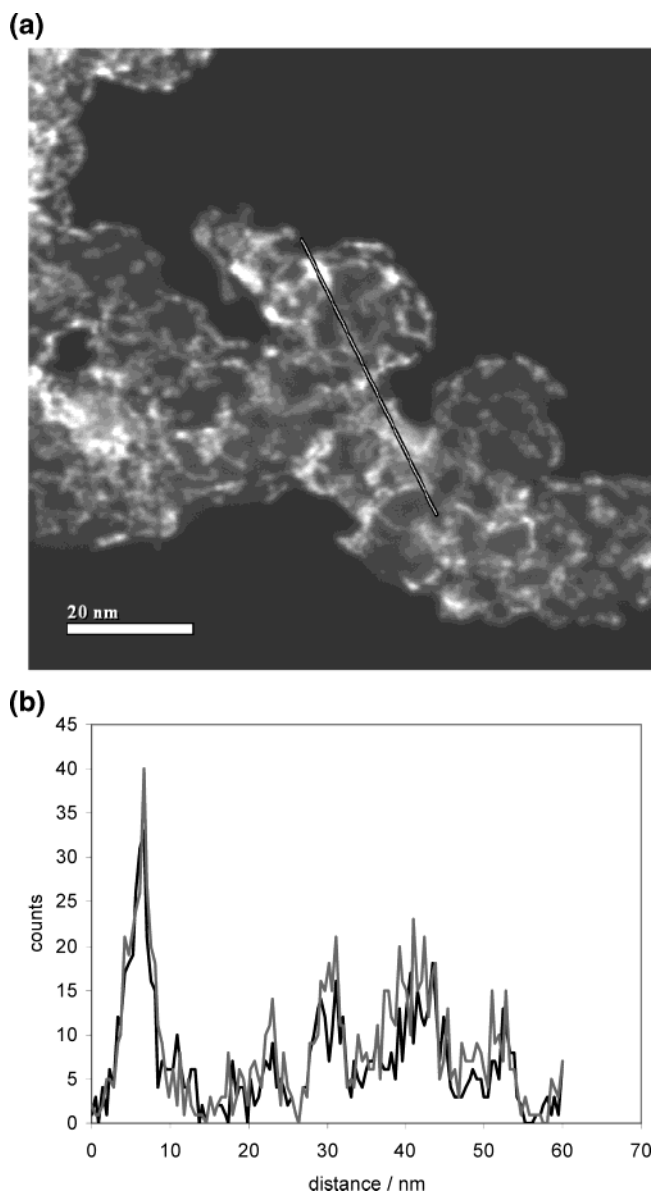


**Figure 7.** Part a shows an annular dark field image taken in the scanning TEM (STEM) mode for a 20 wt % Pt and 10 wt % Ru catalyst supported on Vulcan XC-72R. The PtRu catalyst was synthesized using a 0.071 M NaOH solution, resulting in a 2 nm average PtRu particle size. The white line indicates the region scanned for the EDS data shown in (b). The black line in (b) shows the counts for Pt, while the gray line shows the counts for Ru.

TEM (STEM) mode of a 20:10 wt % Pt:Ru catalyst supported on carbon black. The catalyst was synthesized using a 0.071 M NaOH solution. The bright white features seen in this figure arise from the PtRu noble metal catalysts. Branched-like structures resulting from agglomeration of particles are observed. The average particle size is seen to be around 2 nm, consistent with the particle size and size distribution analysis carried out individually (see Table 1 and Figure 2). Elemental profiles taken across two different regions of these catalysts and obtained from energy-dispersive X-ray spectroscopy (EDS) are shown in Figure 7b. The EDS profile corresponds to the scanned region, indicated by the white line shown in Figure 7a. The EDS counts are shown directly. The counts are proportional to the atomic concentration of Pt and Ru and reflect changes in the Pt and Ru atomic concentrations over the scanned distance. However,

these counts do not yield the actual Pt:Ru atomic concentrations, as they are not normalized. The EDS profiles show no clear signs of segregation; that is, no particles consist of only Ru or Pt. However, because of the low counts, the experimental error is significant and the analysis is not sensitive to small variations.

It is noteworthy that HRTEM images were obtained that confirmed the crystalline nature of the PtRu catalysts. However, due to the limited resolution of the TEM, no additional information such as lattice spacing values was extracted from the data and the HRTEM images are not shown and discussed here.

**Electro-oxidation Characteristics of CH<sub>3</sub>OH.** Carbon-supported PtRu catalysts electrodes were prepared on Au foils, as described in the Experimental Section. Electrodes consisting of small amounts (ca. 0.02 mg of Pt and ca. 0.01 mg of Ru) of catalysts and forming thin catalyst layers were prepared in this manner. The use of thin layer electrodes ensures that all catalyst sites are accessible to the reactant, that is, that true catalytic activities rather than mass transport limitations of the reactant within the catalyst layer are studied. Figure 8a and b shows the CH<sub>3</sub>OH oxidation activity at 60 °C for electrodes made using carbon-supported PtRu particles of 2 nm average size, that is, synthesized using a 0.071 M NaOH solution. Electrochemical data for this particular catalyst are shown here, as studies carried out in parallel work showed this catalyst to exhibit high CH<sub>3</sub>OH oxidation activity per catalyst weight. For comparison, the CH<sub>3</sub>OH oxidation activities for two commercially available catalysts (Alfa Aesar and E-TEK, Inc.) are also shown in Figure 8

a. All electrodes were prepared in the same manner, and catalyst loadings of 20 wt % Pt and 10 wt % Ru on carbon were used in all cases. The CVs suggest that PtRu catalysts prepared in this work exhibit better CH<sub>3</sub>OH electro-oxidation activities than the two commercial catalysts tested, as higher CH<sub>3</sub>OH oxidation currents are observed at lower potentials. In parallel work, current-transient measurements at constant potential were carried out over 8 h periods, showing that the catalytic advantage of these PtRu catalysts is maintained. Each CV curve shown is the average of three different electrodes prepared using a particular catalyst type and loading. In the case of the Alfa Aesar and E-TEK, Inc. catalysts, the same *i*-*V* curve shapes were obtained for multiple electrodes. However, two distinctively different *i*-*V* curve types were obtained for the PtRu catalysts prepared in this work, as shown in Figure 8b. The CV type shown in the black curve in Figure 8b (which is identical to the CV shown in Figure 8a) was observed for ca. 70% of the prepared electrodes made of PtRu catalysts of particle size larger than 1.2 nm, while the gray curve shown in Figure 8b was observed for ca. 30% of these electrodes. In the case of the electrodes prepared using smaller than 1 nm PtRu catalysts, the latter CV type, that is, the gray curve in Figure 8b, was dominant at ca. 90% observed. The electrodes prepared in this work are made of very small amounts of catalysts, and hence the fact that two distinctively different CV types are observed for the prepared PtRu catalysts possibly indicates that the individual electrodes consist of PtRu catalysts of two characteristically different properties, such as, for example, a mainly PtRu alloy versus separate Pt and Ru phases.

### Concluding Remarks

In this study, a simple and rapid synthesis method for the preparation of PtRu colloids that can be subsequently deposited

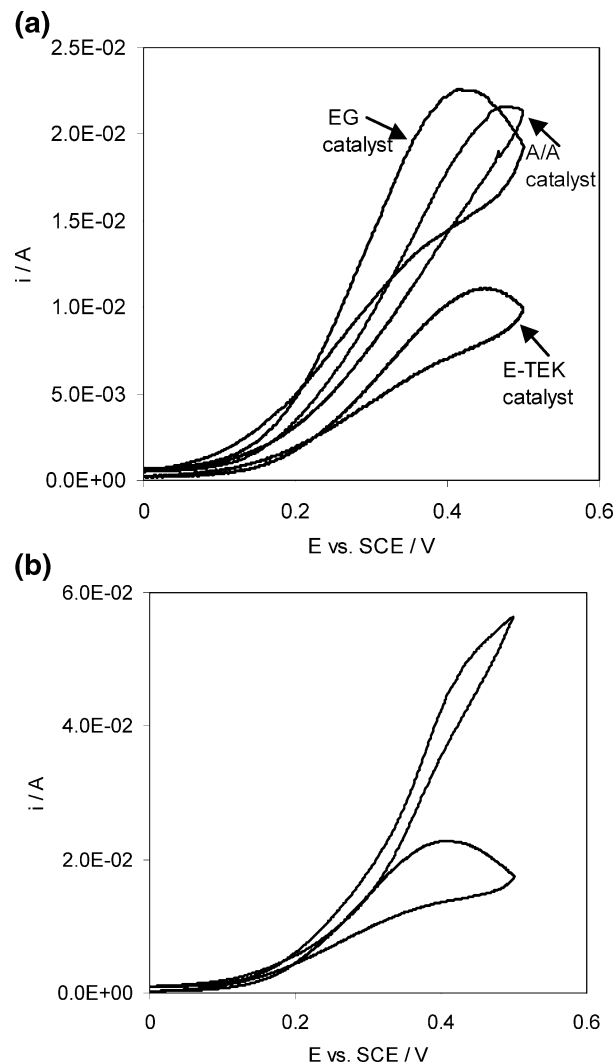


**Figure 8.** Cyclic voltammograms recorded at  $10 \text{ mV s}^{-1}$  in  $0.5 \text{ M CH}_3\text{OH} + 0.5 \text{ M H}_2\text{SO}_4$  solutions at  $60 \text{ }^\circ\text{C}$ . Part a shows the CVs for a 2 nm average particle size PtRu catalyst synthesized in this work (labeled as EG catalyst), a PtRu catalyst from Alfa Aesar (A/A catalyst), and a PtRu catalyst from E-TEK, Inc. Part b shows the two CV types observed for the 2 nm average particle size PtRu catalysts prepared in this work. In all cases, 20 wt % Pt and 10 wt % Ru on Vulcan XC-72R catalysts loadings were used.

on suitable substrates such as high surface area carbon blacks has been introduced. PtRu catalysts of a nominal and final composition of 50:50 atom % Pt:Ru were studied. It has been shown that the size of the PtRu catalyst particles can be varied in the range of 0.7–4 nm. The formation of the particles involves the reduction of the Pt and Ru precursor salts by the solvent, ethylene glycol, which in turn is oxidized. The oxidation of ethylene glycol is shown to mainly result in glycolic acid or, depending on the synthesis solution pH, the glycolate anion. The glycolate anion acts as a stabilizer for the PtRu colloids, and its concentration, and hence the resulting PtRu particle size, is controlled via the synthesis solution pH. The fact that the size of the PtRu catalyst particles is varied via the pH and glycolate concentration only, that is, maintaining other experimental conditions constant, appears to result in PtRu catalyst compositions that are independent of the catalyst particle size. This was supported by XRD data obtained for carbon-supported PtRu catalyst particles larger than 1.2 nm. The XRD data suggest that Ru is partially (ca. 15 atom %) dissolved in

the fcc Pt lattice and that a separate hexagonal Ru phase is also present. The composition of the less than 1 nm PtRu catalysts appears to be different, and the catalyst particles possibly consist of separate Pt and Ru phases. It is possible that alloy formation of such very small particles that consist of only a few atoms (<40) that are mainly (>80%) surface atoms is very difficult or may even not be possible for the PtRu system.<sup>21</sup>

Initial studies showed that particular PtRu catalysts prepared in this work display better CH<sub>3</sub>OH electro-oxidation activities than two commercial catalysts tested. This shows the potential of these synthesis methods to generate improved catalyst formulations for low-temperature methanol fuel cells. However, it needs to be emphasized that long-term studies in real fuel cell systems need to be carried out for these catalysts. Also, the synthesis method will need to be further optimized to gain

(21) LePage, Y. Program Clusurf, ICPET; National Research Council of Canada, Ottawa, 2002.

a better understanding and control of the PtRu alloy versus separate Pt and Ru phase formation.

It is noteworthy that this synthesis method is also attractive because the glycolate stabilizer is a simple organic molecule that can be oxidatively removed either electrochemically or by oxidative heat treatment at temperatures as low as 160 °C.<sup>15</sup> Heat treatments at these “low” temperatures free up valuable catalyst sites without resulting in changes of the PtRu catalyst properties.<sup>5,15</sup>

**Acknowledgment.** We thank I. Sproule and S. Moisa (NRC, Ottawa) for the XPS analysis and D. Wang (NRC, Ottawa) for the TEM analysis. P. L’Abbe’s (NRC, Ottawa) assistance for the preparation of the glass cells used in this work is also greatly acknowledged. Financial support from a joint NRC/Helmholtz grant and the NRC fuel cell program is also gratefully appreciated.

JA0495819